Classical Computing in Nuclear Magnetic Resonance

MARTA ROSELLÓ-MERINO, MATTHIAS BECHMANN,
ANGELIKA SEBALD, SUSAN STEPNEY

Department of Chemistry, and Department of Computer Science
University of York

As part of our longer term research objective of using the complex structure and dynamics of matter to perform non classical *in materio* computation, we show how to use NMR to perform *classical* computation. We describe three different approaches of using NMR to implement a single universal logic gate, and a circuit of these gates combined in parallel and in sequence that implement other logic gates, including various optimisations, and, in one case, a half-adder circuit. We then show how the three approaches are just specific instances of a more general approach set in a rich parameter space, and discuss how this parameter space might be exploited for more sophisticated computations.

Key words: NMR, *in materio* computing, universal gates, trajectories

1 INTRODUCTION

Nuclear Magnetic Resonance (NMR) is used as an implementation technology for quantum computation. Here we instead use NMR to perform *classical* computation. This is part of a longer term research objective of using the complex structure and dynamics of matter to perform non classical *in materio* computation [1, 23]. Our long term aim is to discover the potential and context of NMR as non-standard computing substrate; we are starting with a classical approach in order to understand the capabilities and performance of the medium and the technology.

The paper is structured as follows. First, we provide the necessary background to the NMR physics and technology needed for the rest of the paper, and we explain how our approach differs from the traditional use of NMR for quantum computation. Then we describe the NMR parameter space, and focus on the very small portion of it used so far. Next we describe three different approaches of using solution-state NMR to implement a single universal logic gate, and a circuit of these gates combined in parallel and in sequence that implement other logic gates, including various optimisations. We round this off by showing how one of these approaches scales, in the implementation of a half-adder circuit. Then we show how the three approaches are just specific instances of a more general approach set in a rich parameter space, provide an initial classification of this space, uniquely defined outputs, etc, and discuss how this parameter space might be exploited for more sophisticated computations. We conclude with a few suggestions on how this approach might be extended to non-classical *in materio* computation. Full experimental details are provided in Appendix B.

2 SOME BASIC PRINCIPLES OF NMR

2.1 Nuclear spins

NMR relies on the intrinsic property spin S of microscopic particles such as protons or electrons. In quantum mechanics, spin is associated with a magnetic moment; for atomic nuclei the proportionality factor γ is the gyromagnetic ratio. γ is a specific quantity for a given isotope, and the vast majority of elements in the periodic table are made up of at least one isotope with a non-vanishing nuclear spin [13]. Here we consider only nuclei with $S = 1/2$.

When placed in a homogeneous magnetic field $\mathbf{B}_0$, precession around the main direction of the magnetic field results from the interaction of these magnetic moments with the field (the Zeeman interaction), at a frequency $\omega_0 = -\gamma \mathbf{B}_0$ (the Larmor frequency).

In this picture any, say, ^{1}H nuclei would have the same precession frequency, regardless of the chemical nature of the compound in which they reside. There are additional, smaller, effects that determine the final outcome of NMR experiments and which are responsible for the huge success of solution-state NMR as an analytical method over the past several decades. Atomic nuclei are embedded in molecules and are in contact with the electrons forming chemical bonds. The electronic environment varies slightly in different, inequivalent parts of molecular structures, and nuclear spins residing in different such molecular sites experience slightly different local mag-

netic fields, because the surrounding electrons tend to shield the nuclei from the effects of the external magnetic field in a site-specific manner. This effect was discovered in the early days of NMR when physicists, aiming to determine the gyromagnetic ratio for some isotopes, noticed that they obtained slightly different results, depending on the chemicals used for the measurement [6, 19, 20]. This NMR effect is known as chemical shielding (*CS)*, and it represents an interaction between the nuclear spins, the surrounding electrons, and the magnetic field $\mathbf{B}_0$.

In addition, there are interactions between nuclear spins, especially when in close proximity to each other. A nuclear spin senses the presence of another nuclear spin nearby in the form of dipolar coupling. Dipolar coupling can take the form of a direct through-space interaction (*D*) and as such is proportional to the inverse cube of the internuclear distance, r^{-3}. Dipolar coupling can also be mediated by bonding electrons, that is, by electrons shared between nuclei. In this form it is an indirect interaction (*J*) and its value is a complicated function of molecular structure.

All NMR interactions $\lambda = CS, D, J$ are anisotropic, having a magnitude and a direction, and can be described by second rank tensors A^λ. The following conventions apply to the uniform treatment of all these anisotropic NMR interactions [10]. The isotropic part A^λ_{iso}, the anisotropy δ^λ, and the asymmetry parameter η^λ relate to the principal elements of the interaction tensor A^λ according to $A^\lambda_{iso} = (A^\lambda_{xx} + A^\lambda_{yy} + A^\lambda_{zz})/3$; $\delta^\lambda = A^\lambda_{zz} - A^\lambda_{iso}$; and $\eta^\lambda = (A^\lambda_{yy} - A^\lambda_{xx})/\delta^\lambda$ with $\mid A^\lambda_{zz} - A^\lambda_{iso} \mid \geqslant \mid A^\lambda_{xx} - A^\lambda_{iso} \mid \geqslant \mid A^\lambda_{yy} - A^\lambda_{iso} \mid$. η^λ can assume values between 0 and 1. Assignment of the principal axes is always such that the direction of its *z*-axis corresponds to the principal value, A^λ_{zz}, furthest away from A^λ_{iso} whereas its *y*-axis corresponds to the principal value, A^λ_{yy}, closest to A^λ_{iso}. Together, the anisotropy δ^λ and the asymmetry parameter η^λ describe the shape of the interaction tensor A^λ. It is commonly in solid matter that fully anisotropic NMR interactions are displayed.

Here we take the greatly simplifying step in restricting our discussion to the NMR of small molecules dissolved in non-viscous liquids at ambient conditions. Under these conditions, rapid and isotropic molecular tumbling in solution reduces the NMR interactions to their isotropic averages. Direct dipolar coupling is not directly observable as its isotropic average is zero; only ω^{CS}_{iso} and ω^{J}_{iso} remain directly observable. Figure 1 sketches a hypothetical example of the effect of *J* coupling.

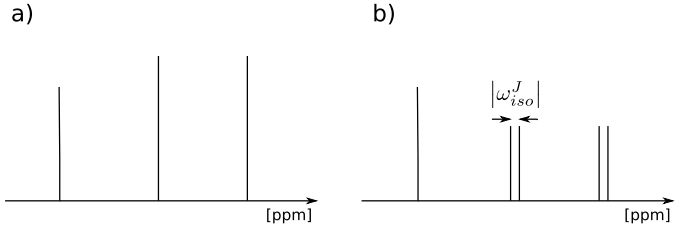

FIGURE 1
A sketch of a hypothetical solution-state ^{1}H NMR spectrum of a small molecule with three different hydrogen sites (a) in the absence of *J* coupling; (b) in the presence of *J* coupling between two of the ^{1}H nuclei in the molecule, leading to a splitting $\mid \omega_{iso}^{J} \mid$ of two of the three resonances into doublets.

2.2 NMR and quantum computing

J-coupled networks of spin-1/2 isotopes form the basis of quantum computing implementations in solution-state NMR by manipulating and exploiting the entangled states represented by the network of mutually coupled spins [4, 5, 9, 15].

Here, however, we take another simplifying step and drop *J* coupling from the agenda: we consider spin systems where ω_{iso}^{CS} is the only NMR interaction present.

2.3 Manipulating spins

Basic experiment

The first step in any NMR experiment is the establishment of net nuclear spin magnetisation by placing the sample in a homogeneous magnetic field $\mathbf{B}_0$, reaching thermal equilibrium according to the Boltzmann distribution of the, loosely speaking, 'spin up' and 'spin down' states. This net magnetisation is conveniently described in a rotating frame of reference, where the frame rotates around the main $\mathbf{B}_0$ direction at the same angular velocity as the Larmor precession of the nuclear spins, ω_0. In this rotating frame the net magnetisation appears static and, in our case, may be represented by a vector $\mathbf{S}$ along the $\mathbf{B}_0$ direction, symbolising the equilibrium magnetisation (see figure 2).

Application of a radiofrequency (rf) pulse at the appropriate frequency and perpendicular to $\mathbf{B}_0$ tips the magnetisation vector $\mathbf{S}$ away from the *z*-direction toward the *xy*-plane. The flip angle depends on the amplitude and duration of the pulse; it is common to refer to, for example, $\pi/2$ (90°) or π (180°)

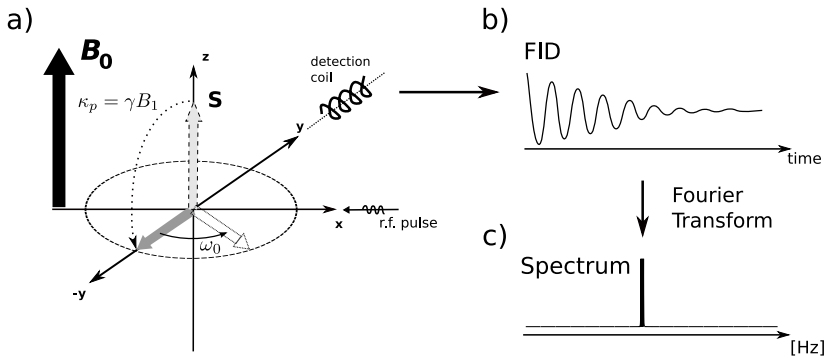

FIGURE 2
Manipulating spins and observing results: (a) the magnetic field and magnetisation vectors; (b) the observed free induction decay; (c) the Fourier-transformed spectrum.

pulses. After the pulse, the *xy*-magnetisation starts to dephase; the decay is monitored in the receiver coil as a *free induction decay* (FID).

Finally, after Fourier transformation of this time-domain data, the NMR spectrum is obtained in the frequency domain. The decay of the signal in the time domain occurs with a characteristic time constant (relaxation time T_2) and equilibrium magnetisation is restored with another characteristic time constant (relaxation time T_1). $T_1 = T_2$ in our scenario of small molecules in non-viscous solvents at ambient conditions.

Spin echo

Rf pulses may be applied not only to equilibrium magnetisation. Consider the magnetisation vector **S** tipped to the xy-plane and aligned with, say the y-direction. If we apply a $180°$ rf pulse with phase ϕ_x, **S** will be flipped to the $-y$-direction (see figure 3). In short: by combining $180°$ rf pulses applied to xy-magnetisation with suitable delays, one can create echoes of the NMR signal at specific points in time. These concepts of π rotations are a fundamental building block in numerous NMR experiments, usually referred to as 'spin echo' or 'Hahn echo' [11, 13].

Pulse profile

Consider the excitation profiles associated with rf pulses of different shapes and amplitudes [8, 17], figure 4. Note that we can obviously choose between

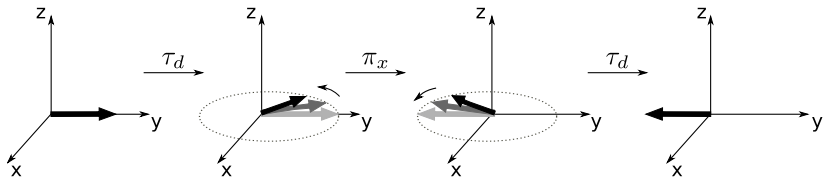

FIGURE 3
Spin-echo experiment employing intervals τ_d of free evolution of spin vectors $\mathbf{S}$ and a π_x pulse applied to xy-magnetisation. During the first τ_d interval the spin vectors $\mathbf{S}$ evolve (rotate) according to their frequency offset from the transmitter frequency (rotating resonance frame): on resonant is static (light grey); slightly off resonant is slow (dark grey); further off resonant is faster (black). The π_x-pulse inverts the y-components of the $\mathbf{S}$ vectors, inverting their order, causing a complete refocusing of the spin vectors after a second interval τ_d, and a spin-echo is formed.

exciting a narrow frequency band with, for example, a Gaussian-shaped pulse ("selective" excitation) and exciting a wider frequency range by applying hard pulses ("non-selective" excitation).

Magnetic field gradient

Consider the effects of an additional magnetic field gradient along the z-direction of $\mathbf{B}_0$. This is symbolised in figure 5. Without the z-gradient, in a homogeneous sample in a homogeneous field $\mathbf{B}_0$ the Larmor frequencies / resonance conditions for identical particles/spins are identical throughout the sample volume. In the presence of the z-gradient, the resonance conditions vary as a function of space and according to the gradient strength, adding $\mathbf{B}_g$ and $\mathbf{B}_0$.

$\mathbf{B}_g$ could be either a static gradient or a pulsed gradient (switched on and off). In either case, a magnetic field gradient allows the molecular mobility in solution to be monitored (different molecules diffusing through the sample at different rates) by carrying out experiments which label the NMR response of a molecule with its dynamic history. This is usually achieved by using pulsed gradients at specific times in a NMR pulse sequence.

Otherwise, field gradients enable us to define spatial regions in the sample (the basis of magnetic resonance imaging, for example in medical applications). This is achieved by using gradients both during the NMR pulse sequence and the following data acquisition.

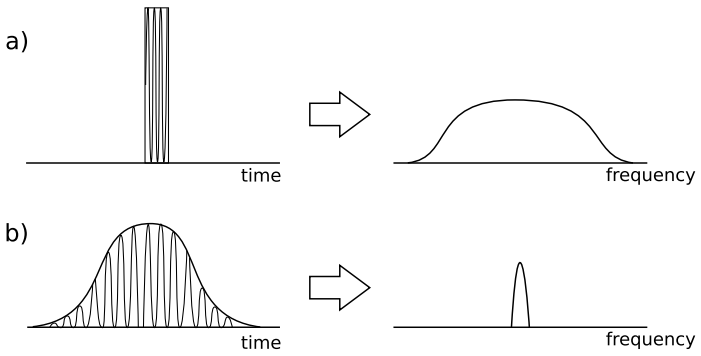

FIGURE 4
Excitation profile (a) of a high amplitude, rectangular pulse (a “hard pulse”); (b) of a low-amplitude, Gaussian-shaped pulse

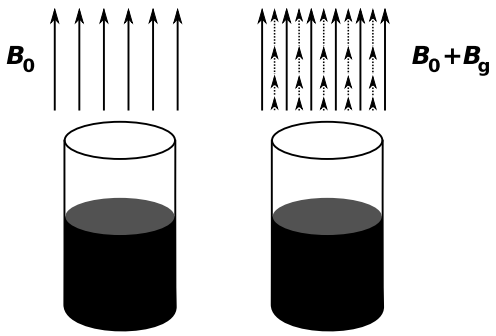

FIGURE 5
A magnetic field in the absence (left) and presence (right) of a magnetic field gradient.

3 THE NMR PARAMETER SPACE

Having introduced the basic NMR concepts, we recast these in the context of a NMR parameter space for the construction of logic gates. Even having restricted our NMR operational base to the simplest of possible NMR cases, we have a rich parameter space to work with. In solution-state NMR options for defining input exist in the NMR experiment itself, in external experimental conditions, and in the set of chemical and physical properties of the samples chosen.

The NMR experiment itself includes rf pulses, delays, and data acquisition. Data acquisition is characterised by its duration τ_a, the phase of the receiver ϕ_a, the observation frequency ω_a, and options for coherence selection by phase cycling [7, 14]. Various different delays of different durations τ_d can be implemented in a pulse sequence (for example, in a spin echo experiments). A versatile selection is provided by the rf pulses which are characterised by their amplitude κ_p, duration τ_p, frequency ω_p, and phase ϕ_p. In addition, the shape of rf pulses can be varied, as can the number of pulses applied in a sequence.

Experimental conditions primarily concern the magnetic field(s) involved: the homogeneity $\partial B_0/\partial r$ and stability $\partial B_0/\partial t$ of the external magnetic field, as well as the properties of pulsed (or static) additional magnetic field gradients $\partial^2 B_g/\partial r \partial t$.

Choice of sample is another rich field of potential choices to define input parameters. In terms of NMR properties, we can work with single- or multiple-component samples, yielding spectra with single or multiple NMR resonances, depending on the chemical shielding values ω_{iso}^{CS}. In addition, selective, full, or random isotope-labelling broadens this choice. Different chemical compounds and sample preparations, as well as the use of different isotopes, lead to different values of the T_1 and T_2 relaxation times. Physical properties of samples such as self-diffusion $\partial c(r,t)/\partial t$ in solution make bulk properties of samples available for the choice of input parameters.

Output parameters occupy a similarly rich space. The orientation of the magnetisation after a rf pulse sequence ($x, y, z, -x, -y, -z$; $ax + by + cz$), the FID itself, integrated signal intensities, the number of resonances detected and/or their relative intensities, all offer a flexible basis for defining suitable output parameters.

4 SOLUTION-STATE NMR IMPLEMENTATIONS OF LOGIC GATES

We have briefly introduced all necessary ingredients for the implementation of logic gates by NMR. The options include the construction of extended gates and circuits, where the wiring of a more complicated circuit is implemented by a script in the spectrometer software which carries forward output from one experiment as input to the next. Here we discuss three specific implementations of logic gates and more extended circuits that take advantage of various different choices of input and output parameters from the NMR parameter space. Figure 6 shows the pulse sequences used in these examples; figure 7 summarises the logic input and output parameter assignments for each of the implementations. Specific experimental details are given in Appendix B.

Output. In all the approaches considered below, we chose the integrated spectral intensity as the output parameter. The value of this integral depends on whether the detected signal is "absorptive", "dispersive", or has zero amplitude, which in turn depends on the relative phases of rf pulses, receiver and starting magnetisation.

Dispersive and zero-amplitude signals yield a zero integral; absorptive signals a non-zero integral (see figure 8). Because of noise, "zero" means below and "non-zero" above a certain threshold value; see Appendix B for details of the threshold used in the experiments.

A zero integral is interpreted as bit value 0, a non-zero integral as 1.

5 APPROACH 1: DIFFUSION ORDERED SPECTROSCOPY (DOSY) RELATED EXPERIMENTS

By exploiting diffusion properties of different chemical compounds in solution, this implementation rests on a bulk property of the sample (**D**iffusion **O**rdered **S**pectroscop**Y**: DOSY [12]).

We chose a pulsed gradient spin echo (PGSE) sequence [2] for this approach to the implementation of logic gates (figure 6a). The implementation of a two-input universal logic gate was carried out with a two-component sample. These two components, chloroform and polymethyl siloxane, dissolved in deuterated chloroform, produce two single, well separated signals in the ^{1}H NMR spectrum of the sample (figure 9).

The two components greatly differ in their diffusion properties: chloroform has a much higher diffusion coefficient than polymethyl siloxane and,

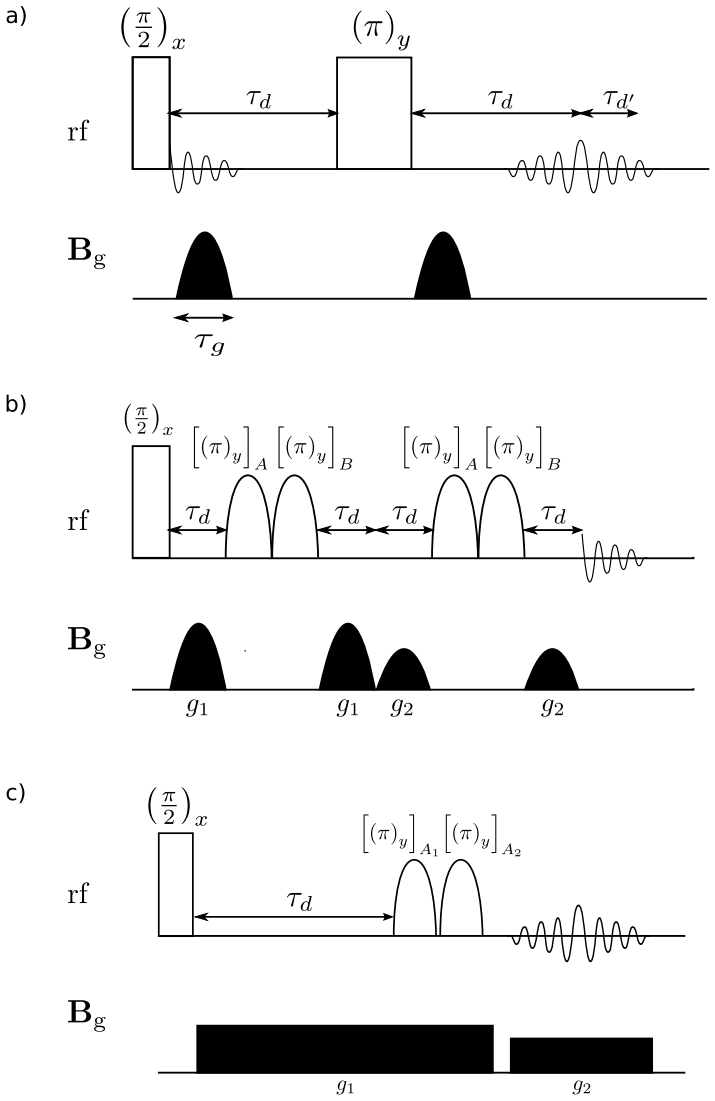

FIGURE 6
Basic pulse sequences used on the different approaches to the implementation of logic gates: (a) a pulsed-gradient spin echo (PGSE) sequence; (b) a double pulsed-field-gradient echo (DPFGE) sequence; (c) a spin-echo-based slice selection sequence.

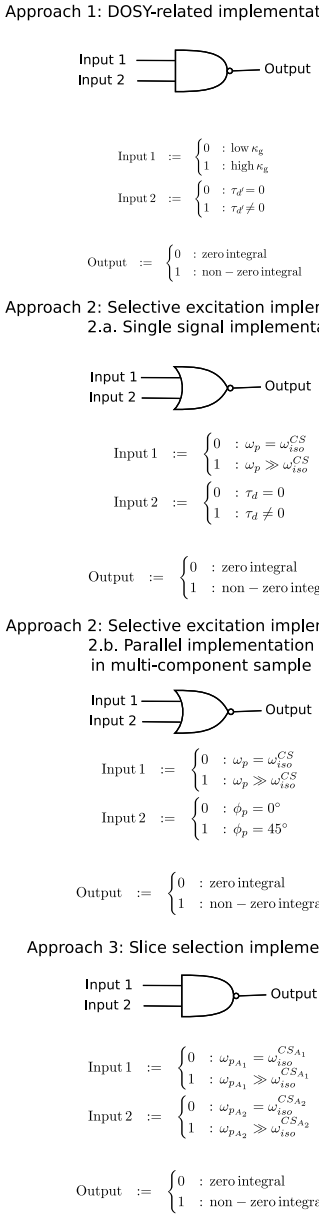

FIGURE 7
Summary of the logic input and output parameter assignment for each of the logic gates implemented within this section. Approaches 1 and 3 implement a NAND gate; approach 2 implements a NOR gate.

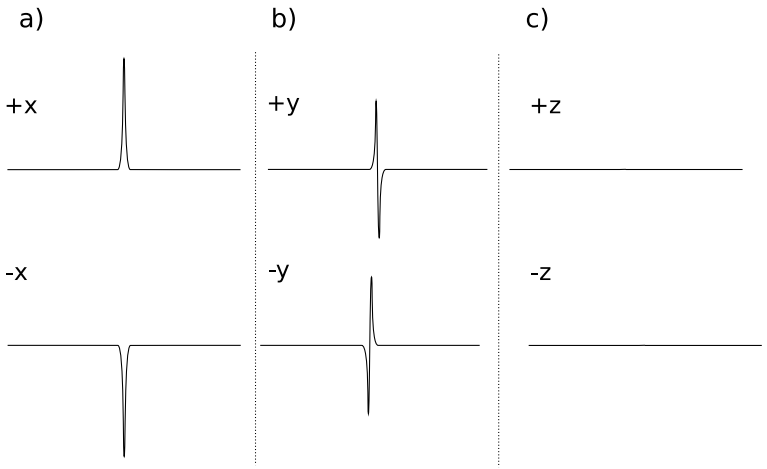

FIGURE 8
NMR frequency spectra obtained when detecting the signal along the the $+x$-axis and the magnetisation pointing along (a) $\pm x$-axis: absorption; (b) $\pm y$-axis: dispersion; (c) $\pm z$-axis: zero

accordingly, we expect strongly differing responses of the two components to the presence of pulsed gradients. This is because the trajectories of the faster-diffusing compound spread over a wider range of space, and therefore of resonant frequencies in the magnetic field gradient. The ^{1}H NMR signal of chloroform is expected to be much more strongly attenuated by diffusion than the ^{1}H NMR signal of the polymer molecule polymethyl siloxane [3, 12].

Input parameter one: gradient strength. Gradient strength (κ_g) and duration (τ_g), as well as the duration of the pre-acquisition delay (τ_d) in the PGSE experiment are all parameters that can be modified experimentally to alter the extent of the effect of diffusion on the intensity of an echo signal (figure 6a).

Here we chose to fix both τ_g and τ_d and to modify the gradient strength κ_g. With a low gradient strength, the effect of diffusion on both echo signal intensities is minimal as only a very small space-dependent phase shift is then introduced. High gradient strength causes more extensive space-dependent dephasing. With bulk diffusion randomly altering the position of the spins in the sample, for a more rapidly diffusing compound, this results in incomplete

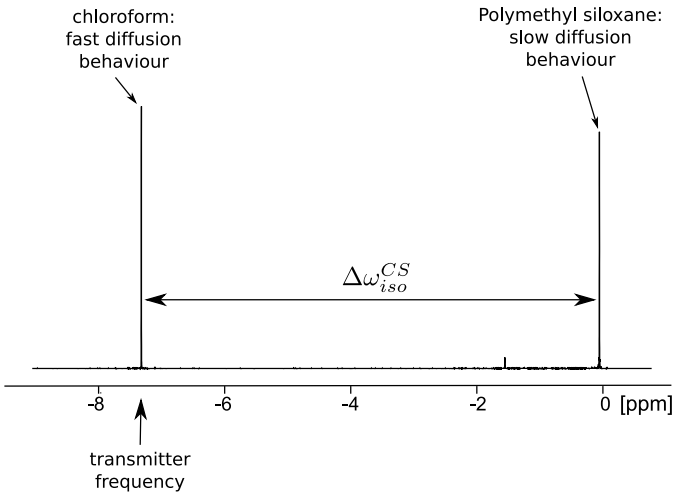

FIGURE 9
^{1}H-NMR spectrum of a mixture of chloroform and polymethyl siloxane, where the rotating frame frequency is that of the chloroform signal. The magnetization arising from chloroform is therefore static in the rotating frame whereas the polymethyl siloxane magnetization rotates with a $\Delta\omega_{iso}^{CS}$ frequency.

refocusing of the magnetisation and a strong attenuation of the resulting echo signal.

So gradient strength represents our first input. A strong gradient (strong enough to dephase the chloroform ^{1}H signal, but not strongly affecting the ^{1}H signal of polymethyl siloxane) represents first input bit value 1; a weak gradient (leaving both ^{1}H resonances largely undisturbed) represents bit value 0.

Input parameter two: delay. As the second input, we chose an experimental parameter which affects only the ^{1}H NMR signal of the slower diffusing component. In order to achieve this, the transmitter frequency of the rf pulses was set on resonance for the chloroform ^{1}H resonance. This resonance, therefore, always appears static in the rotating frame and only the ^{1}H magnetisation of the polymethyl siloxane evolves in this frame in the *xy*-plane. This off-resonance signal develops a phase shift in the rotating frame, depending on the difference in resonance frequency $\Delta\omega_{iso}^{CS}$ between the two components. We exploited this phase shift between on- and off-resonance signals as our second input by delaying the start of the data acquisition by $\tau_{d'}$ (figure 6a). If we choose the point in time when a 90° phase shift has developed to start the data acquisition, the off-resonance signal will be dispersive if the on-resonance signal is absorptive (see figures 8, 10b). The dispersive signal has a zero integrated intensity.

So data acquisition delay represents our second input. The presence of the delay $\tau_{d'}$ in the PGSE experiment represents second input bit value 1; its absence represents bit value 0.

Output. We chose the total integrated spectral intensity as the output parameter. A zero total integral is interpreted as bit value 0, a non-zero total integral as 1.

Results. Figure 10 shows our experimental spectra of ^{1}H NMR PGSE experiments, acquired with the four possible combinations of the input parameters κ_g and $\tau_{d'}$. The corresponding truth table is that of the NAND gate.

Possibilities for parallelism

In this implementation, each PGSE experiment corresponds to one logic gate. Therefore, in order to construct more complicated logic gates, based on combinations of several NAND gates, as many PGSE experiments as NAND gates

Input 1 (gradient strength, κ_g)	Input 2 ($\tau_{d'}$)	Output
Low (0)	$\tau_{d'} = 0$ (0)	1
Low (0)	$\tau_{d'} \neq 0$ (1)	1
High (1)	$\tau_{d'} = 0$ (0)	1
High (1)	$\tau_{d'} \neq 0$ (1)	0

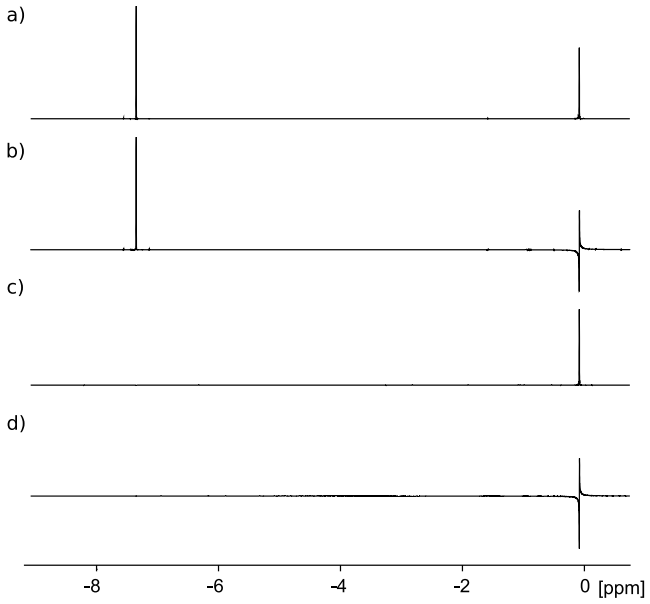

FIGURE 10
Truth table of the NAND logic gate, as implementated by a DOSY-related experiment. Spectra are shown for experiments acquired with each of the four possible input combinations: (a) 0 0; (b) 0 1; (c) 1 0; (d) 1 1.

need to be executed. We did implement such gates in this manner (for instance, XOR and AND; data not shown) but there is little prospect for parallelism with the DOSY-based approach. If one wanted to carry out simultaneous gates in DOSY experiments, one would have to opt for multi-component samples. While it is perfectly possible to fully control absence/presence and relative phases of the ^{1}H NMR signals of just two components with vastly different diffusion coefficients, this is not a realistic option for multi-component samples made up from compounds covering a range of diffusion rates. It would probably be necessary to use sequential parameter control, and not much would be gained over multiple experiments. It is for this reason that we now abandon the DOSY approach and explore further options.

6 APPROACH 2: SELECTIVE EXCITATION

6.1 Selective excitation experiments: first steps with single-component samples

This implementation uses the absence or presence of an on-resonance 90° pulse as an input controlling the presence or absence of a signal in the NMR spectrum. Applying an off-resonance rf pulse and introducing an appropriate delay τ_d the phase of the resulting signal can be varied between absorptive and dispersive (figure 11).

Input parameter one: pulse on/off resonance. A 90° pulse applied on resonance represents the first input bit value 0; no 90° pulse (that is, rf amplitude $\omega_p \gg \omega_{iso}^{CS}$) represents bit value 1.

Input parameter two: delay. A delay $\tau_d = 0$ represents the second input bit value 0; a delay τ_d causing a 90° phase shift represents bit value 1.

Output. We again chose the total integrated area as the output parameter for this implementation. A zero total integral is interpreted as bit value 0, a non-zero total integral as 1.

Results. Figure 12 shows NMR spectra obtained for the four possible combinations of inputs. It can be seen that only one signal is now needed to implement a logic gate. The truth table is that of the NOR gate. It is obvious that in a single-signal situation it does not matter if the pulse applied is hard or soft (i.e. selective), as the same result will be achieved with both

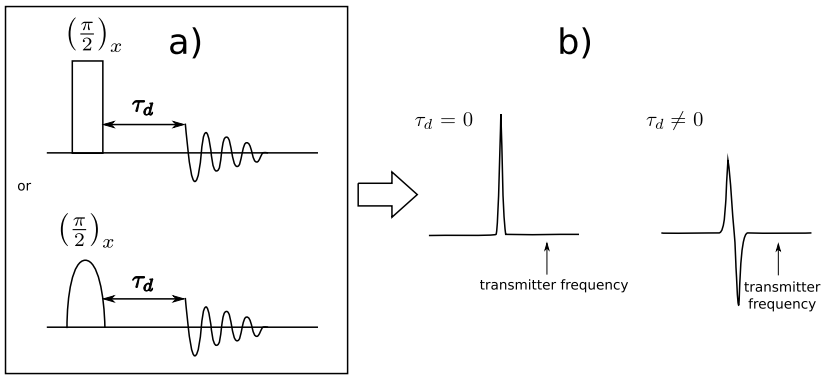

FIGURE 11
The phase of an off-resonance signal can be controlled by varying the starting point of the acquisition time after a 90°pulse is applied to the equilibrium magnetisation. If the signal is phased so that an absorptive peak is obtained for $\tau_d = 0$, an appropriate duration of τ_d can be introduced so that the off-resonant magnetisation acquires a 90°phase shift, producing a dispersive peak.

types of rf pulses. With this single-component implementation, possibilities for parallelism are limited but now we have room for improvements by using multi-component samples in conjunction with selective pulses.

6.2 Selective excitation experiments: multi-component samples

Selective pulses can be independently applied at different transmitter frequencies for independent control of the presence or absence of different signals. The phase of the selective pulses can also be modified, resulting in different phases of the signals produced. For example, exciting the equilibrium magnetisation with a $(90°)_x$ pulse will produce a signal that is 90° out of phase with respect to that obtained with a $(90°)_y$ pulse. Using pulse phases enables independent signal-phase control, which allows us to abandon phase control using delays which we used in the previous approaches, but which is not practical for multi-component systems. Using the rf pulse off-set and phase parameters, two-input logic gates can now be implemented in parallel by using a multi-component sample and assigning each gate to a signal.

When it is desired to select more than one signal within one pulse sequence, a double pulsed-field-gradient echo (DPFGE) [18] sequence can be used (figure 6b). In this experiment, equilibrium magnetisation is initially

Input 1 (selective pulse offset)	Input 2 (delayτ_d)	Output
$\omega_p = \omega_{iso}^{CS}$ (0)	$\tau_d = 0$ (0)	1
$\omega_p = \omega_{iso}^{CS}$ (0)	$\tau_d \neq 0$ (1)	0
$\omega_p \gg \omega_{iso}^{CS}$ (1)	$\tau_d = 0$ (0)	0
$\omega_p \gg \omega_{iso}^{CS}$ (1)	$\tau_d \neq 0$ (1)	0

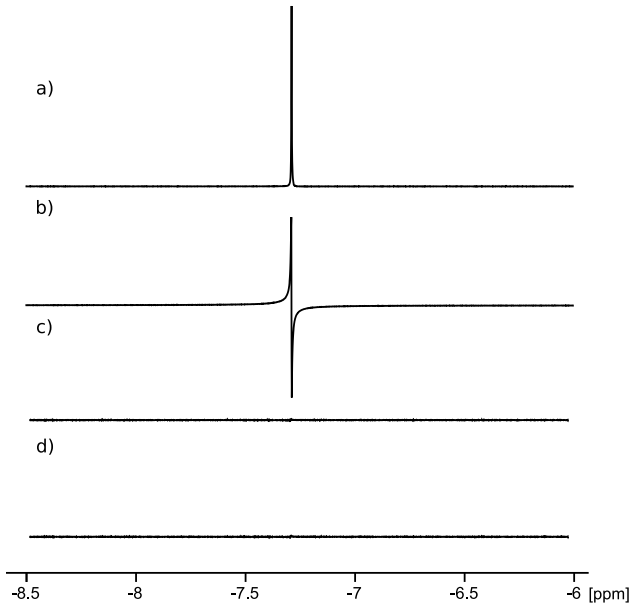

FIGURE 12
Truth table of the NOR gate, as implemented by selective excitation and delay-based signal phase control in a single component sample. Spectra for the four possible input combinations are shown: (a) 0 0 ; (b) 0 1 ; (c) 1 0 ; (d) 1 1

brought to the *xy*-plane by a non-selective 90° pulse, followed by two gradient spin echoes. Normally hard 180° pulses would be used for refocussing, but now are replaced by trains of selective 180° pulses, composed of as many pulses as signals are necessary to be selected. The first gradient spin echo refocuses the signals at the chosen frequency (or frequencies) while gradients dephase the magnetisation that is not inverted. The second echo refocuses the chemical shielding evolution that occurs during the experiment and eventually produces a spectrum of in-phase signals.

Input parameter one: offset. The offset of the selective pulses ω_p represents one of the inputs for this approach to the implementation of logic gates. If the offset is such that the selective pulse is applied on resonance for the frequency of a given component, then a signal is obtained. A large offset causes the selective pulse to be applied outside the NMR spectral range and does not excite any magnetisation, therefore not producing a signal.

A selective pulse applied on-resonance represents the first input bit value 0; a selective pulse with a sufficiently large offset represents bit value 1.

Input parameter two: phase. The second input parameter is the phase of the selective pulse, ϕ_p, which, as we have seen, affects the phase of the resulting signal. If in the DPFGE experiment, the selective π pulses in the first half of the pulse sequence are shifted by $\phi_p = 45^\circ$, this results in a 90° out-of-phase signal. Not applying the phase shift ϕ_p to the selective π pulses yields an absorptive signal.

A non-phase-shifted selective π pulse represents the second input bit value 0; a phase-shifted selective π pulse represents bit value 1.

Output. The output is the integrated spectral intensity at the chosen resonance frequency. A zero integral is interpreted as bit value 0, a non-zero integral as 1.

Scaling up and achieving parallelism

Unlike in the DOSY-based approach where each experiment implemented a single logic gate, now several logic gates can be implemented in a single DPFGE pulse sequence. All we need is a sample giving rise to as many reasonably well resolved resonances as are needed for the simultaneous implementation of logic gates. In addition, the pulse sequence needs to be set up such that it includes the necessary number of selective pulses.

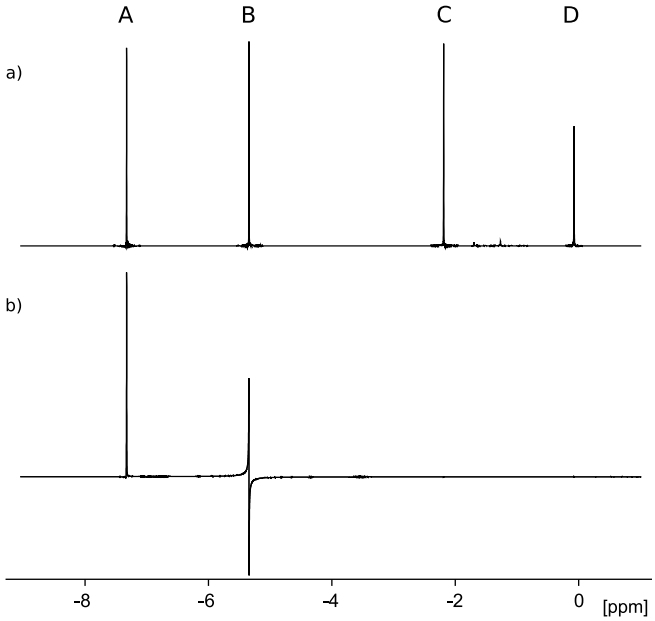

Input 1 (selective pulse offset)	Input 2 (selective pulse phase)	Output
$\omega_{p_A} = \omega_{iso}^{CS_A}$ (0)	$\phi_{p_A} = 0^o$ (0)	1
$\omega_{p_B} = \omega_{iso}^{CS_B}$ (0)	$\phi_{p_B} = 45^o$ (1)	0
$\omega_{p_C} \gg \omega_{iso}^{CS_C}$ (1)	$\phi_{p_C} = 0^o$ (0)	0
$\omega_{p_D} \gg \omega_{iso}^{CS_D}$ (1)	$\phi_{p_D} = 45^o$ (1)	0

FIGURE 13
(a) ^{1}H-NMR spectrum of mixture of (A) chloroform, (B) dichloromethane, (C) acetone and (D) polymethyl siloxane in deuterated chloroform; (b) a DPFGE experiment recorded with the same sample where each of the four possible input combinations assigned for the implementation of a logic gate have been implemented on a different signal : chloroform (0 0), dichloromethane (0 1), acetone (1 0) and polymethyl siloxane (1 1). The implemented truth table is that of the NOR logic gate.

Figure 13a shows the conventional ^{1}H NMR spectrum of a mixture of four compounds (chloroform, dichloromethane, acetone and polymethyl siloxane). The ^{1}H NMR DPFGE experiment now requires four selective pulses for the handling of four independent components in the ^{1}H NMR spectrum in order to implement four logic gates simultaneously. This is shown in figure 13b where four NOR logic gates, one for each of the four possible input combinations, are implemented, one with each of the spectral components.

As shown in figure 13b, each gate is associated with a signal with specific inputs (offset and phase) of the shaped pulse that selects it. It is therefore straightforward to scale up this implementation to execute a large number of logic gates in a single experiment, as the control of the presence/absence and/or phase of each signal is completely independent. (In the DOSY Approach 1, multicomponents are a problem because their diffusion properties are being used; here multicomponents are usable because their resonance properties are being used.)

As the NOR logic gate is universal and can be used to construct all other basic logic gates, the ease with which parallelism is achieved in this approach can be used to reduce execution times in NOR-based logic gates and other complex circuits. The limits to the extent of parallelism achievable are given by the availability of suitable multicomponent samples, by spectral resolution and by the duration of the trains of selective pulses in the DPFGE experiments. T_1 and T_2 relaxation limit the useful duration of any selective excitation pulse sequences. In fact, long relaxation times in NMR are beneficial in this circumstance, unlike the case when using NMR in its role as analytical tool.

Example: an AND gate built from three NOR gates

Figure 14 shows how an AND gate can be constructed from three NOR gates. It also shows a step-by-step description of the implementation of the gate. The first two gates can be run in parallel, which is possible with the selective excitation approach described above. The last NOR gate needs to be run in a different experiment, as its inputs depend on the outputs of the previous two NOR logic gates. Therefore, two experiments are needed to complete the AND logic gate. The sample used for this implementation needs to give rise to a minimum of two signals for the desired parallelism to be achievable.

It can also be noted that in this circuit the two first logic gates can have only 0 0 or 1 1 input values. In practice, the two inputs for each gate can be set manually for the initial experiment. Another possibility is to write a script for the spectrometer software so that given one of the inputs (for example, the

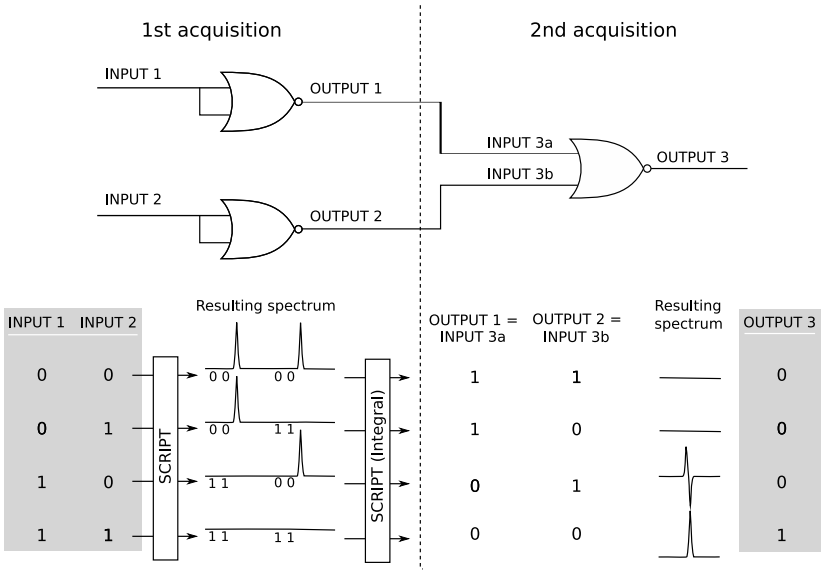

FIGURE 14
The construction of an AND logic gate based on NOR universal logic gates (top) and step-by step description of the spectra obtained for the two experiments needed to complete the implementation for each of the four possible input combinations (bottom).

pulse offset), the other input (for example, pulse phase) is changed accordingly to establish either a 1 1 or 0 0 situation. This would reduce set-up time, and can be considered to be a "compiler optimisation" step.

A script is also needed so that integration is carried out on each of the selected frequency ranges at the end of the first experiment and their value is translated into the inputs for the final acquisition. In this sense, the script acts as the "wires" of the circuit (performing a fixed signal transduction operation), and is not performing any actual computation (again, it is a compile-time function).

The integrated area of the spectrum obtained in the last experiment indicates the output of the completed AND gate.

7 APPROACH 3: SLICE SELECTION EXPERIMENTS

To achieve parallelism, the implementation of logic gates based on selective pulses that we have described in the previous section relies on having a sample made of a mixture of components that produce signals with adequate spectral resolution. This can be difficult to obtain when many signals are needed to achieve a high degree of parallelism. It may be useful to devise implementations of logic gates that would also allow some degree of parallelism but could be carried out on a single-component sample. In that sense, slice-selection NMR experiments are a good starting point.

Figure 6c shows a basic 1D spin-echo-based slice selection experiment [2, 16] which we use on a single component sample (chloroform in deuterated chloroform). Initially a non-selective 90° pulse is applied to the equilibrium magnetisation. This brings the magnetisation to the *xy*-plane where it rotates with its characteristic frequency ω_{iso}^{CS}. A magnetic field z-gradient g_1 is then switched on, causing the rotating frequency to acquire a phase shift dependent on the position along the z-axis of the sample during a delay τ_d. This creates a frequency profile of the sample as ω_{iso}^{CS} now depends on position by sampling the combined effects of $\mathbf{B}_0$ and $\mathbf{B}_g$ (see figure 5). Slices of such a distribution of resonance frequencies can be extracted with selective 180° pulses. The magnetisation inverted with such selective pulses will be refocused (spin echo) whereas the rest of the magnetisation, outside the excitation profile of the selective pulse, will continue to dephase, not giving rise to any detectable NMR signal.

As the experiment is performed on a single-component sample, if no gradient was present during the acquisition time, the refocused magnetisation would appear as a single signal at frequency ω_{iso}^{CS} in the resulting spectrum.

In that case, the intensity of the signal would be related to the total width of the selected slices. The presence of another magnetic field gradient g_2 during acquisition allows the separation of signal contributions arising from different slices in the sample (g_2 and g_1 may or may not be equal). The shape, amplitude and duration of g_1 are critical to define the frequency range over which slices can be selected. Wider frequency ranges, caused by stronger gradients, will obviously result in less intense signals for equal slice widths.

NMR spectra obtained with this type of experiment are the Fourier transform of an echo signal and hence display oscillating phase behaviour. If absorptive signals are desired, spectra need to be displayed in magnitude mode (absolute intensity mode). This means that any phase information is lost. Therefore, in this implementation, instead of controlling the absence/presence and the phase of a single NMR signal (as in approach 2), we now control the absence/presence of two NMR signals for the construction of a two-input logic gate.

Input parameters: selective pulse offsets. For the implementation of a single two-input logic gate, the pulse sequence (figure 6c) includes two selective pulses, ω_{p_A}, each of them associated with a different sample slice, and the selective pulse offsets are chosen as the two inputs parameters.

A selective pulse that excites the ^{1}H magnetisation in a sample slice (the location of which is a function of g_1) represents first/second input bit value 0; a selective pulse applied outside the ^{1}H resonance frequency range of the sample represents bit value 1.

Output. The output is defined as the integrated area of the spectrum. A zero integral is interpreted as bit value 0, a non-zero integral as 1.

Results. Figure 15 shows spectra for the four possible combinations of these logic inputs. The truth table obtained is that of the NAND logic gate. Being universal, it is possible to construct all other basic logic gates with this approach.

Scaling up and achieving parallelism

Parallelism can be achieved by increasing the number of selective pulses applied within the pulse sequence. Each pair of addressed sample slices would be a NAND logic gate, and several could be implemented within a single pulse sequence. However, scaling up is not as straightforward as when using selective excitation in a multicomponent sample, as every time a new selective

Input 1 (selective pulse 1 offset)	Input 2 (selective pulse 2 offset)	Output
$\omega_{p_{A_1}} = \omega_{iso}^{CS_A}$ (0)	$\omega_{p_{A_2}} = \omega_{iso}^{CS_A}$ (0)	1
$\omega_{p_{A_1}} = \omega_{iso}^{CS_A}$ (0)	$\omega_{p_{A_2}} = \omega_{iso}^{CS_A}$ (1)	1
$\omega_{p_{A_1}} \gg \omega_{iso}^{CS_A}$ (1)	$\omega_{p_{A_2}} \gg \omega_{iso}^{CS_A}$ (0)	1
$\omega_{p_{A_1}} \gg \omega_{iso}^{CS_A}$ (1)	$\omega_{p_{A_2}} \gg \omega_{iso}^{CS_A}$ (1)	0

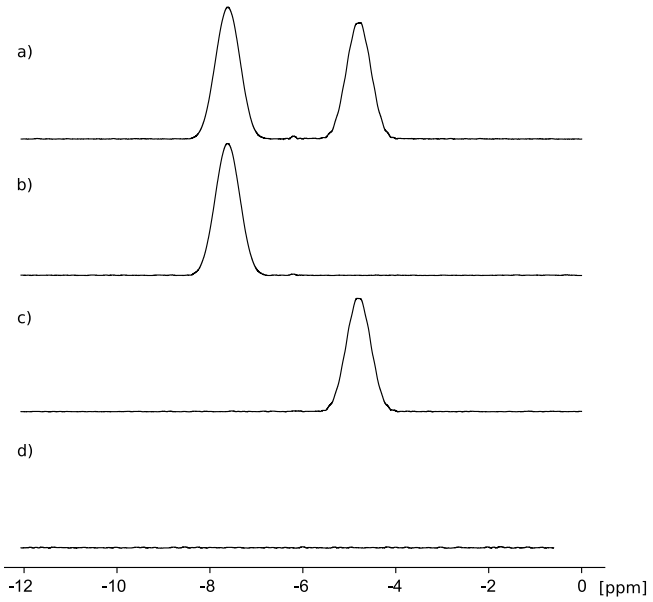

FIGURE 15
Truth table of the NAND gate, as implemented by a spin-echo-based slice selection experiment in a single component sample (chloroform in deuterated chloroform). Spectra for the four possible combination of inputs are shown: (a) 0 0; (b) 0 1; (c) 1 0; (d) 1 1.

pulse is introduced in the pulse sequence careful optimisation of experimental parameters (e.g. delay τ_d, starting point and duration of acquisition) is needed. The number of gates that can be run in parallel is restricted, among other factors, by the duration of the selective pulses. To select a larger number of slices from a certain sample profile, pulses need to be made longer to excite narrower frequency ranges. As in the previous approach, T_1 and T_2 relaxation limit the useful duration of the selective experiment. Increasing the gradient strength g_1 increases the width of the resonance-frequency profile over the sample and can make it possible to increase the number of slices selected. However, the intensity of the resulting signals will be less for identical slice thicknesses. The compromise between these factors (gradient strength κ_g and pulse duration τ_p) is what ultimately dictates the extent of parallelism that can be achieved with this implementation.

8 A HALF-ADDER CIRCUIT

Here we show how approach 2b, selective excitation with multi-component samples, can be used to implement a complex circuit: a half adder circuit implemented from NOR gates.

All the implementations described above can be used to implement a circuit such as the half-adder. Approaches 2 and 3, which allow parallelism, reduce the execution time with respect to approach 1. Selective excitation in a multi-component sample is chosen for this example, as it is the most straightforward of the two implementations for the level of parallelism and sample complexity needed when implementing a single half-adder circuit.

The half-adder circuit is slightly more complicated than a basic logic gate. It performs the addition of two one-bit binary numbers, producing a sum and carry values. Figure 16a shows the half-adder circuit, which is formed by connecting XOR and AND logic gates. This circuit can be constructed solely from universal NOR gates if the XOR and AND gates are substituted by their NOR-based equivalents. The resulting circuit is shown in figure 16b.

Note that part of the NOR-based circuits for the XOR and AND gates are identical, and even have the same inputs in the half-adder circuit. Making use of this fact the half-adder circuit can be simplified (figure 17, top) to a NOR-based circuit that is similar to a NOR-based implementation of an XOR logic gate. The only difference is that the carry value is read out directly from the output of one of the intermediate NOR logic gates, as shown in figure 17, and the sum corresponds to the XOR gate output.

A sample that gives rise to a minimum of two ^{1}H NMR signals is needed

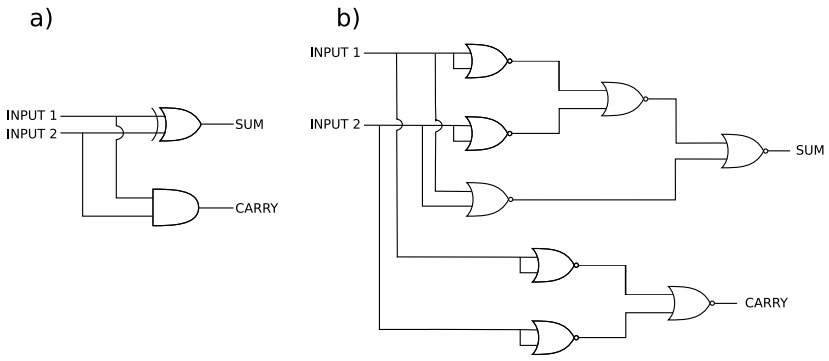

FIGURE 16
Half-adder circuit (a) constructed from an XOR and an AND gate; (b) constructed from only NOR gates.

for the DPFGE-based [18] implementation of a half-adder with the NOR-based circuit. This is because gates 1 and 2 can be run in parallel, and so can be gates 3 and 4. Three separate experiments are needed to complete the implementation. The first experiment is identical to the first acquisition for the NOR-based AND gate (described above). The inputs correspond to the two one-bit binary numbers that are to be summed. In the second experiment, one of the NOR gates (4) is run with its two inputs corresponding to the inputs of gates 1 and 2. The inputs for gate 3 are given by the integrated area of the signals produced by gates 1 and 2 in the first experiment. The output of gate 3 is read as the carry of the sum. The third and final experiment contains only one NOR logic gate whose inputs are given by the integrated area of the signals produced by gates 3 and 4 in the second experiment. The output of gate 5 is the sum of the two one-bit binary numbers.

9 TIMINGS

An NMR experiment can be segmented into the following parts:

1. pulse sequence: the time during which rf pulses and delays are applied to the spin system in order to create the spin state

2. acquisition time: the time during which the NMR signal FID is detected until it has completely decayed

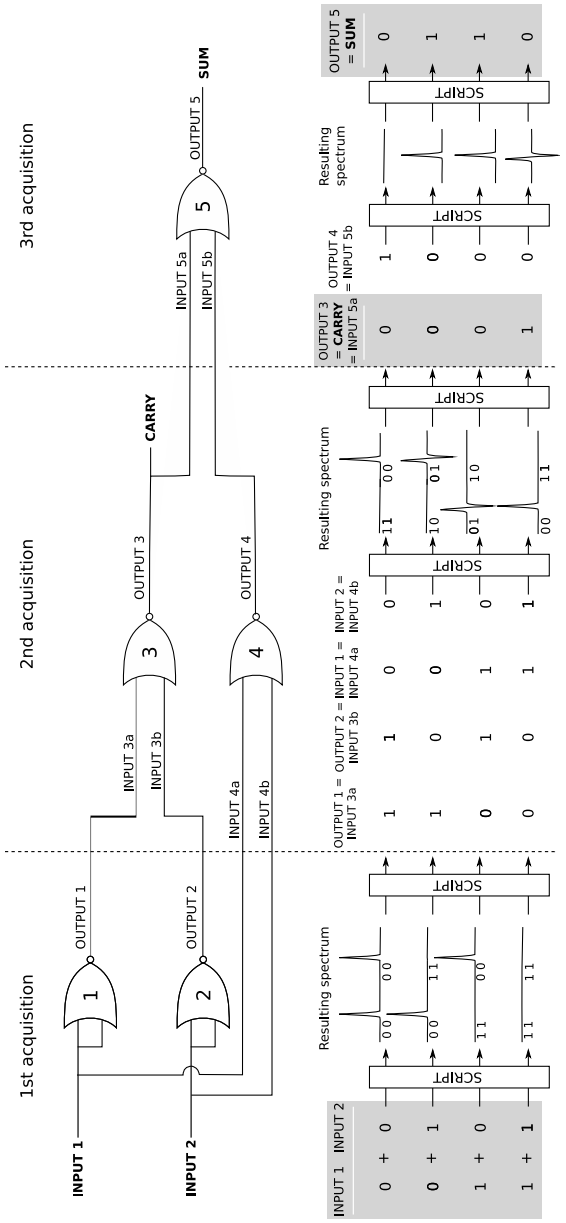

FIGURE 17
Simplified NOR-based half-adder circuit (top) and a step-by step diagram of the inputs and outputs for each of the three DPFGE experiments needed to complete it (bottom).

approach	pulse sequence	acquisition	recovery	total
1	802.1 ms	2.8 s	1s	4.6 s
2a	93.7 ms	1.5 s	1s	2.6 s
2b	163.4 ms	2.5 s	1s	3.7 s
3	20.4 ms	23.0 ms	1s	1.0 s

TABLE 1
Experiment times for the individual gates in the various approaches.

3. recovery time: the time during which the system is relaxing to thermal equilibrium (necessary to continue with the next experiment)

The overall time it takes to run a single sequential gate is the sum of these three times. (We include the recovery time even for single gates, for uniformity of comparison, since it is the critical component in multiple sequential experiments used to implement circuits.)

The results for our experiments are shown in table 1. The half adder takes 7.3 s in total to execute.

10 DISCUSSION AND OUTLOOK

10.1 Constructing gates

We have demonstrated how to use NMR to execute logic gates. Three methodologically distinct, but very basic, NMR experiments have been explained together with their interpretation in the field of logical operations. In a more general picture we now discuss the peculiarities of using NMR to implement logic gates. A logic gate in its general form can be seen as consisting of three parts: input — gate operation — output. The operational flow chart of a general NMR logic gate is shown in figure 18.

A typical gate has one, two, or more inputs. Without loss of generality we restrict ourselves to gates with two inputs; the important universal gates are of this kind. For the NMR version of a logic gate the input to the NMR experiment is generally all of the NMR parameters introduced (see earlier) at their default values. These values are defined by the actual NMR implementation (for example, the three implementations discussed above). In order to control the gate operation it is necessary to choose a pair from these parameters as the actual two inputs and map values of these to a two-state logic. It is generally permitted to pick any suitable pair of parameters to construct a

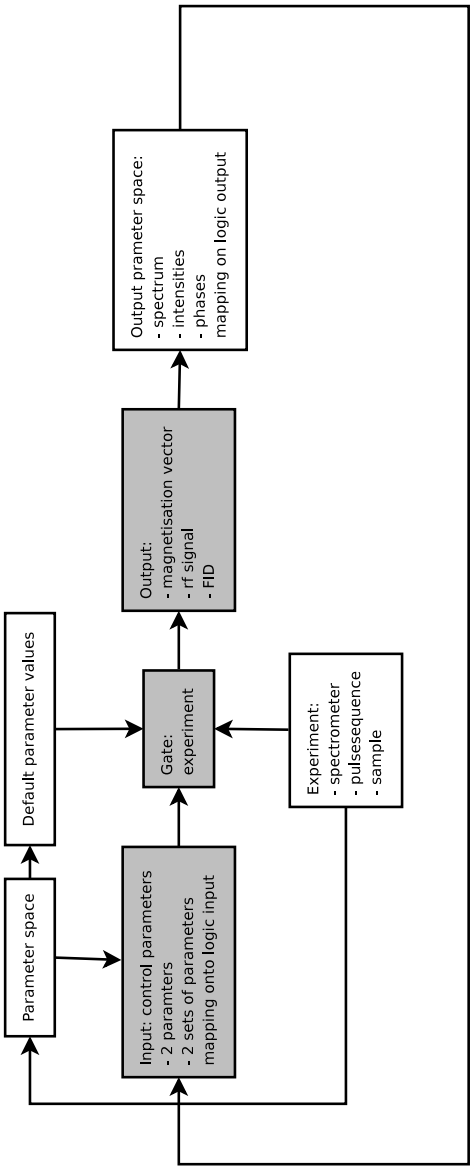

FIGURE 18
Schematic of the operation of a general NMR logic gate.

gate; it would even be possible to construct the two members of the input pair from a group of parameters changing simultaneously. In an abstract view the gate is dependent on the total NMR parameter space, but is driven only by the parameters from a small subspace. The huge size of the NMR parameter space and the enormous scope for combinations of parameters allows for a plethora of possible input pairs. Here we examine which kind of gates can be implemented using which kinds of input parameters, giving a classification of the parameters and their mapping to logic input.

The actual gate operation is conducted by the NMR experiment, which consists of a spectrometer executing an rf pulse program on a chosen sample by interpreting the input parameters. As demonstrated above, there is a large number of possible NMR experiments, achievable by changing the rf pulse sequence, the sample, or the spectrometer hardware. All this adds to the possibilities of implementing various gate operations.

The output of the NMR experiment, and therefore the gate, is basically the trajectory of the magnetisation vector as detected by the magnetic induction in the receiver coil, typically recorded as an oscillating electric time signal. This output is mapped onto a logic two-state set according to variations of the time signal for various inputs. Changes in oscillation frequency, amplitude, phase, and duration are typical effects. It is common in NMR to analyse the oscillatory and phase behaviour of the time signal by a frequency analysis using Fourier transformation. This yields frequency-domain spectra displaying resonance lines. Therefore, a typical mapping onto a logic output is the appearance or disappearance of a resonance line, a change in its phase, etc.

10.2 Classification of parameter space

In the following we analyse the possibility of constructing any of the possible 16 two-input logic gates by a chosen pair of input parameters and a suitable output parameter. We analyse and characterise the difference in physical nature of the various input parameters (amplitude, frequency, duration, phase, etc.) and their influence on possible gate implementations.

One of the simplest NMR experiments is a $\pi/2$-pulse sequence (see figure 19) applied to a sample consisting of a single spin species, displaying only a single value ω_{iso}^{CS}. In this kind of experiment the magnetisation vector is tipped from its equilibrium position along $\mathbf{B}_0$ by an angle of $\pi/2$ into the xy-plane resulting in a spectrum with a single Lorentzian shaped resonance line. A $\pi/2$ pulse is the basic building block of all NMR pulse experiments. The $\pi/2$-pulse sequence can be parametrised by 5 parameters. All other parameters take default values. Four parameters control the $\pi/2$ rf pulse κ_p, ω_p, τ_p,

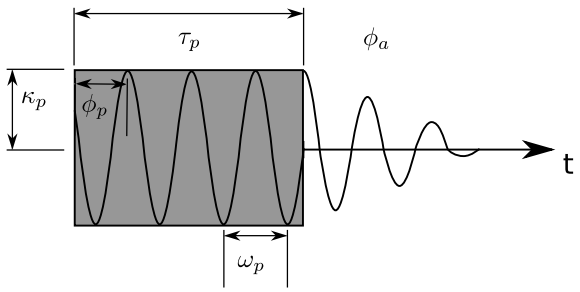

FIGURE 19
$\pi/2$-pulse sequence with the relevant experimental parameters

ϕ_p, and one parameter controls the phase of the acquisition ϕ_a. They take the values $\kappa_p = \kappa_p^{\pi/2}$, $\omega_p = \omega_{iso}^{CS}$, $\tau_p = \tau_p^{\pi/2}$, $\phi_p = x$ and $\phi_a = -y$. The flip angle of the pulse is given by

$$\beta = \kappa_p^{\pi/2}\tau_p^{\pi/2} = \frac{\pi}{2} \tag{1}$$

Mapping logic states to input and output parameters: $\pi/2$-pulse experiment applied to z-magnetisation. Picking κ_p, τ_p as the two NMR parameters to control the logic gate inputs, a possible mapping of these parameters to the logic states 0 and 1 is

$$\text{Input } 1 := \begin{cases} 0 & : \kappa_p = 0 \\ 1 & : \kappa_p = \kappa_p^{\pi/2} \end{cases} \tag{2}$$

$$\text{Input } 2 := \begin{cases} 0 & : \tau_p = 0 \\ 1 & : \tau_p = \tau_p^{\pi/2} \end{cases} \tag{3}$$

The experimental effect of altering these parameters is only to flip the magnetisation vector to the xy-plane if both inputs are 1, and hence a signal is detectable. If any of the inputs is zero no signal can be detected.

A possibility is to map the integrated area of the obtained spectrum $S(\omega)$ to 0 and 1 as

$$\text{Output} := \begin{cases} 0 & : \int_{\omega_a}^{\omega_b} S(\omega)\mathrm{d}\omega = 0 \\ 1 & : \int_{\omega_a}^{\omega_b} S(\omega)\mathrm{d}\omega \neq 0 \end{cases} \tag{4}$$

The resulting truth table of this configuration reveals a logic AND gate.

The mapping of the input parameters κ_p, τ_p to the logic states 0 and 1 shown in equations (2) and (3) is not unique but allows for a total of 2×2 permutations. Analysis of these four mappings reveals the four logic gates AND, $>$, $<$,* and NOR. Applying the same reasoning to the mapping in equation (4) for the output parameter provides additional configurations for OR, $\geq$, $\leq$ and NAND gates. These are logic gates that have precisely one 1 (or precisely one 0) as output in their truth table.

Note that identical gate operations can be obtained by starting with $-y$-magnetisation instead of remapping the output from working with z-magnetisation (see Appendix A).

A different logic behaviour can be achieved when the parameters ϕ_p, ϕ_a are chosen as input and all the other parameters take values typical for a $\pi/2$-pulse experiment. The logic gate input can then be mapped like

$$\text{Input}\,1 := \begin{cases} 0 & : \phi_p = x \\ 1 & : \phi_p = y \end{cases} \tag{5}$$

$$\text{Input}\,2 := \begin{cases} 0 & : \phi_a = x \\ 1 & : \phi_a = -y \end{cases} \tag{6}$$

The experimental effect of altering input 1 is to rotate the magnetisation vector about either the x- or y-axis hence placing the magnetisation vector along $-y$- or x-axis respectively after the $\pi/2$-pulse. Input 2 controls along which axis the magnetisation is detected. Choosing an output mapping identical to the one given in equation (4), the respective truth-table is describing a XOR gate. Applying the permutations to the input mapping as described before, there are again 2×2 permutations possible; however, the four resulting truth tables describe only doubles of XOR and XNOR gates. These are the "balanced" logic gates that have two 1s and two 0s as output in their truth table.

Classification of input parameters. The origin of the different kind of gates constructible from different pairs of experimental input parameters has its origin in the different physical nature of, for example, ϕ_p, ϕ_a on one side and κ_p, τ_p on the other. Comparing the different experimental effects of the two parameter pairs, the following two rules can be formed:

1. if the effect of the first parameter cannot be compensated by a setting

* $(A \leq B) \equiv (A \implies B)$, $(A > B) \equiv \neg(A \leq B) \equiv \neg(A \implies B)$; similarly $(A \geq B) \equiv (B \implies A)$, $(A < B) \equiv \neg(B \implies A)$.

of the second parameter, then AND, $>$, $<$, NOR, OR, $\geq$, $\leq$ and NAND gates can be constructed

2. if the effect of the first parameter can be compensated by a setting of the second parameter, then XOR and XNOR gates can be constructed

Applying these rules to the parameters of the $\pi/2$-pulse sequence the following can be said: the parameters κ_p, ω_p and τ_p are of type amplitude, frequency and duration. Any one of them can control if a pulse is present and, therefore, if magnetisation is tipped into the xy-plane, which afterwards can be detected. These parameters imply rule 1) and therefore we call them *strong* parameters. Switching any one of these parameters off makes the value of all other parameters redundant since the output will be zero in any case. The parameters of type phase ϕ_p, ϕ_a behave differently. Changing the phase of the pulse can be compensated for by also changing the phase of the receiver for data acquisition. This type of parameters we therefore call *weak* parameters.

This classification into strong and weak parameters is not as clear cut as it might seem from the analysis of this simple $\pi/2$-pulse experiment. For example, assuming a pulse sequence consisting of two $\pi/2$-pulses I and II, and choosing the amplitude of the first pulse κ_p^I and the duration of the second pulse τ_p^{II} for gate input, allows for a parameter mapping like

$$\text{Input 1} := \begin{cases} 0 & : \kappa_p^I = 0 \\ 1 & : \kappa_p^I = \kappa_p^{\pi/2} \end{cases} \tag{7}$$

$$\text{Input 2} := \begin{cases} 0 & : \tau_p^{II} = 0 \\ 1 & : \tau_p^{II} = \tau_p^{\pi/2} \end{cases} \tag{8}$$

The results are XOR and XNOR gates. This is despite the previous finding that κ_p and τ_p are classified as strong parameters in a single-pulse NMR experiment. It is not possible to generalise in terms of strong and weak parameters based on single-pulse experiments when considering multi-pulse experiments. In multi-pulse experiments applied to non-coupled spin systems, any rf pulse can always be compensated by a suitable second pulse. Hence, in multi-pulse experiments κ_p and τ_p may now qualify as a pair of weak parameters. It is not generally the case that all two-pulse experiments provide weak parameter pairs as can be seen when analysing the following mapping of ϕ_p^I and τ_p^{II}

$$\text{Input}\,1 := \begin{cases} 0 & : \phi_p^I = 0^\circ \\ 1 & : \phi_p^I = 90^\circ \end{cases} \tag{9}$$

$$\text{Input}\,2 := \begin{cases} 0 & : \tau_p^{II} = 0 \\ 1 & : \tau_p^{II} = \tau_p^{\pi/2} \end{cases} \tag{10}$$

which now is a strong parameter pair. However the set ϕ_p^{II} and τ_p^I provides a weak parameter pair. We tentatively conclude at this point that in general commutation properties, common bases and combinations of these determine the property "weak" or "strong" for a pair of input parameters in multi-pulse NMR experiments. We are currently analysing all the pulse operators and their commutation properties to provide a full mathematical classification of these cases [22].

10.3 Combining gates

The implementation of gates is only the first step in the implementation of a paradigm to accomplish actually useful computation. The rules how a combination of logic gates forming a circuit is able to execute mathematical operations like addition, multiplication or division are well understood. An implementation of logic gates by NMR therefore mirrors the functionality of *in silico* computers.

Contrary to electronically implemented logic gates where the input and output is of the same type (voltage), this restriction does not apply to logic gates employing NMR experiments. Next we analyse which possibilities exist to connect ("wire") gates implemented by NMR experiments to form logic circuits. We distinguish two kinds of configurations by the type of input and output parameters used.

Input type different from output type. As demonstrated in the three experimental approaches above, there exists a wide range of possible NMR experiments that can be used to construct logic gates. In addition, every NMR experiment provides several parameters as potential input for a logic gate. The common characteristic of these implementations is the fact that gate inputs are experimental NMR parameters while the output is chosen to be the result of the experiment. Obviously this makes it conceptually impossible to feed the output of one gate directly to the input of another. The signal transduction between gates, therefore, is a more complex procedure, but does not represent a computation in its own right. A typical signal transduction in this

NMR configuration would consist of the integrated amplitude of a spectral peak controlling e.g. the amplitude of a rf pulse of the following gate.

The advantage of this kind of wiring is that the gate output (e.g. integrated signal intensity) can in principle connect to every NMR parameter in the experiment and is providing a great deal of flexibility. However, this also requires that a complete NMR experiment has to be conducted for every gate operation. Typical durations of NMR-experiment are in the order of seconds and therefore cause a huge performance penalty. This statement neglects the demonstrated possibility of parallel execution of NMR gates as shown above.

Conceptually it would also be possible to confine the detection of the NMR time-domain signal (typically 16k points) to recording of only the first point in the FID whose ordinate is proportional to the integrated spectral area. Signal detection of this kind would reduce the amount of time needed to record the NMR information from the order of seconds to approximately $10\,\mu$s.

Unfortunately, the repetition rate for multiple such single-point NMR experiments is still governed by slow T_1 relaxation, of the order of seconds. This problem could only be circumvented if we could accommodate multiple single-point detections *and* analyses into a single multi-pulse sequence. Contemporary NMR hard- and software permits multiple single-point detection in a single experiment but does not permit the crucial step of analysing the data points and forwarding the result as input for the next step in real time. A fundamental difference would be that subsequent gates would now not be starting from equilibrium magnetisation any more.

Input type equal to output type. Alternatively, we could use the orientation of the spin-magnetisation vector as the input *and* output of a logic gate. This would make it possible to feed the output of one gate directly to the input of subsequent gates, since now the types of input and output are identical. The actual gate experiment would be conducted using the same experimental parameters for a given type of gate throughout, and only the orientation of the input magnetisation would change between gates. The initial input to a circuit of gates would have to be set by using a suitable pulse. This would also make it unnecessary to record the NMR signal after every gate, since the complicated signal transduction and remapping of output to input is avoided.

Since logic gates typically take two inputs it is necessary to have two independent spin vectors S_1 and S_2, and at least two resonances per spectrum. Since the magnetisation vectors can have every possible orientation in space, a subset of these has to be chosen to represent the input states of a logic gate. A possible choice is to consider only magnetisation in the xy-plane with the

Input #		Output		NOR	NAND
In 1	In 2	Out 1	Out 2	> 0	> 1
0	0	1	1	1	1
0	1	1	0	1	0
1	0	0	1	1	0
1	1	0	0	0	0

TABLE 2
Truth table for S_1, S_2 using the mapping of logic input and output according to equations (11)–(13).

orientation angle $\phi_{\mathrm{S_i}}$ of spin S_i mapping to the binary states as

$$\text{Input } 1 := \begin{cases} 0 & : \phi_{\mathrm{S}_1} = +\mathrm{x} \\ 1 & : \phi_{\mathrm{S}_1} = -y \end{cases} \tag{11}$$

$$\text{Input } 2 := \begin{cases} 0 & : \phi_{\mathrm{S}_2} = +\mathrm{x} \\ 1 & : \phi_{\mathrm{S}_2} = -y \end{cases} \tag{12}$$

A gate operation which alters the magnetisation vector while keeping it in the xy-plane would consist of an NMR experiment employing a π pulse with a phase $\phi_p = 135^\circ$. The effect of this $(\pi)_{135}$ pulse is to rotate the $+x$-magnetisation vector to $-y$. To analyse the gate operation a full NMR FID has to be recorded to separate the resonances of the two magnetisation vectors S_1 and S_2 in the spectrum. A suitable mapping of the output to logic states has to be a combination of the signals of the two resonances. One possibility to achieve this is to first assign a binary state to every single spin i resonance as

$$\text{Output } i := \begin{cases} 0 & : \int_{\omega_a}^{\omega_b} S_i(\omega)\,\mathrm{d}\omega = 0;\ \text{along } +x \\ 1 & : \int_{\omega_a}^{\omega_b} S_i(\omega)\,\mathrm{d}\omega \neq 0;\ \text{along } -y \end{cases} \tag{13}$$

and to combine the single spin output state to a combined output by adding the binary states. Obviously this leaves one with three possible outcomes 0, 1 and 2 for the four possible permutations of the two sets of binary states. By choice of a suitable cut-off amplitude the two universal gates NAND and NOR can be constructed (see table 2)

In this way it is possible to execute gate operations by executing one NMR experiment per gate operation. The problem that remains to be solved here is

how to connect the output of one gate to form the input of a subsequent gate in a circuit. This is not entirely straightforward since the output in this implementation consists of actually two spin-vector orientations and it remains to be demonstrated experimentally how to construct a suitable single input [21].

10.4 Conclusions

We have experimental implementations of single and multiple logic gates in solution-state NMR. This demonstrates that NMR can perform classical computation.

The experience that we have gained from these experiments has allowed us to appreciate how the enormous richness of the parameter space might be applied to enable computation. Our next steps are to explore this parameter space more thoroughly, in order (a) to define a rigorous correspondence between parameter choice and the corresponding gates and computations that are implemented; (b) to determine parameters that allow classical circuits to have their "wiring" more naturally implemented by the structure of the experiment; (c) ultimately, to perform non-classical *in materio* computation in NMR, by exploiting its natural properties, as a far-from-equilibrium continuous dynamical system.

REFERENCES

[1] Matthias Bechmann, John A. Clark, Angelika Sebald, and Susan Stepney. (2007). Unentangling nuclear magnetic resonance computing. In *Unconventional Computing 2007, Bristol, UK, July 2007*, pages 1–18. Luniver Press.

[2] P. T. Callaghan. (1993). *Principles of Nuclear Magnetic Resonance Microscopy*. Oxford University Press.

[3] H. Y. Carr and E. M. Purcell. (May 1954). Effects of diffusion on free precession in nuclear magnetic resonance experiments. *Physical Review*, 94(3):630–638.

[4] David G. Cory, Amr F. Fahmy, and Timothy F. Havel. (March 1997). Ensemble quantum computing by NMR spectroscopy. *Proceedings of the National Academy of Sciences*, 94(5):1634–1639.

[5] David G. Cory, Mark D. Price, and Timothy F. Havel. (1998). Nuclear magnetic resonance spectroscopy: an experimentally accessible paradigm for quantum computing. *Physica D*, 120(1-2):82–101.

[6] W. C. Dickinson. (Mar 1950). Dependence of the ^{19}F nuclear resonance position on chemical compound. *Physical Review*, 77(5):736–737.

[7] R. R. Ernst, G. Bodenhausen, and A. Wokaun. (1987). *Principles of Nuclear Magnetic Resonance in One and Two Dimensions*. Oxford University Press.

[8] R. Freeman. (1998). Shaped radiofrequency pulses in high resolution NMR. *Progress in Nuclear Magnetic Resonance Spectroscopy*, 32(48):59–106.

[9] Neil A. Gershenfeld and Isaac L. Chuang. (1997). Bulk spin-resonance quantum computation. *Science*, 275:350–356.

[10] U. Haeberlen. (1976). High resolution NMR in solids. In J. S. Waugh, editor, *Advances in Magnetic Resonance, Supplement 1*. Academic Press.

[11] E. L. Hahn. (Nov 1950). Spin echoes. *Physical Review*, 80(4):580–594.

[12] Charles S. Johnson, Jr. (1999). Diffusion ordered nuclear magnetic resonance spectroscopy: principles and applications. *Progress in Nuclear Magnetic Resonance Spectroscopy*, 34:203–256.

[13] M. H. Levitt. (2008). *Spin Dynamics*. Wiley, 2nd edition.

[14] Malcolm H. Levitt, P. K. Madhu, and Colan E. Hughes. (April 2002). Cogwheel phase cycling. *Journal of Magnetic Resonance*, 155(2):300–306.

[15] David I. Lewin. (2001). Searching for the elusive qubit. *Computing in Science and Engineering*, 3(4):4–7.

[16] Zhi-Pei Liang and Paul C. Lauterbur. (October 1999). *Principles of Magnetic Resonance Imaging: A Signal Processing Perspective*. Wiley-IEEE Press.

[17] A. G. Marshall and F. R. Verdun. (1990). *Fourier Transforms in NMR, Optical, and Mass Spectroscopy: A User's Handbook*. Elsevier.

[18] Teodor Parella, Francisco Sánchez-Ferrando, and Albert Virgili. (November 1998). A simple approach for ultraclean multisite selective excitation using excitation sculpting. *Journal of Magnetic Resonance*, 135(1):50–53.

[19] W. G. Proctor and F. C. Yu. (Mar 1950). The dependence of a nuclear magnetic resonance frequency upon chemical compound. *Physical Review*, 77(5):717.

[20] Norman F. Ramsey. (Jun 1950). Magnetic shielding of nuclei in molecules. *Physical Review*, 78(6):699–703.

[21] Marta Roselló-Merino, Matthias Bechmann, Angelika Sebald, and Susan Stepney. Direct wiring of multi-gate NMR logic circuits; in preparation.

[22] Marta Roselló-Merino, Matthias Bechmann, Angelika Sebald, and Susan Stepney. Pulse operators and their commutation properties in the context of NMR logic gates; to be submitted.

[23] Susan Stepney. (July 2008). The neglected pillar of material computation. *Physica D: Nonlinear Phenomena*, 237(9):1157–1164.

A MAPPING LOGIC STATES TO INPUT AND OUTPUT PARAMETERS: $\pi/2$-PULSE EXPERIMENT APPLIED TO $-Y$-MAGNETISATION

Here we demonstrate how gate operations would operate when initial magnetisation is oriented along the $-y$-axis.

Using a $\pi/2$-pulse experiment applied to $-y$-magnetisation and a parameter set κ_p, τ_p, the mapping of the parameters to the binary states 0 and 1 is

$$\text{Input 1} := \begin{cases} 0 & : \kappa_p = 0 \\ 1 & : \kappa_p = \kappa_p^{\pi/2} \end{cases} \tag{14}$$

$$\text{Input 2} := \begin{cases} 0 & : \tau_p = 0 \\ 1 & : \tau_p = \tau_p^{\pi/2} \end{cases} \tag{15}$$

A starting $-y$-magnetisation enables the logic gates OR, $\geq$, $\leq$ and NAND. Instead of remapping the output in the rather unintuitive way as

$$\text{Output} := \begin{cases} 1 & : \int_{\omega_a}^{\omega_b} S(\omega)\,\mathrm{d}\omega = 0 \\ 0 & : \int_{\omega_a}^{\omega_b} S(\omega)\,\mathrm{d}\omega \neq 0 \end{cases} \tag{16}$$

the input magnetisation can be replaced by $-y$ to achieve the same gate behaviour as before when starting with z-magnetisation.

B EXPERIMENTAL DETAILS

All NMR spectra were recorded at room temperature on a Bruker Avance NMR spectrometer, operating at a Larmor frequency $\omega_0/2\pi = -500.13$ MHz (^{1}H) and fitted with a 5mm TXI ^{1}H-^{13}C/^{15}N probe containing a z-gradient. Bruker Topspin was used as the spectrometer software. Gradient strength percentages are relative to a 100% gradient field strength κ_g = 5 mT cm^{-1}. All field gradients are sine-bell shaped and have a duration of 1 ms, with a recovery delay of 0.2 ms unless otherwise stated. Shaped pulses are derived from a 1000-point, 1%-truncated Gaussian shape. Samples were prepared in 5mm thin-walled glass NMR tubes. The chemical compounds used were chloroform (Aldrich), dichloromethane (Aldrich), acetone (Aldrich) and high vacuum grease (Dow Corning) which is mainly composed of polymethyl siloxane. Their ^{1}H NMR isotropic chemical shielding values are $\omega_{iso}^{CS} = -7.29$ ppm (chloroform), $\omega_{iso}^{CS} = -5.30$ ppm (dichloromethane), $\omega_{iso}^{CS} = -2.16$ ppm (acetone) and $\omega_{iso}^{CS} = -0.01$ ppm (polymethyl siloxane); ω_{iso}^{CS} [ppm] is given relative to ω_{iso}^{CS} (^{1}H) = 0 ppm for an external sample of tetramethyl silane. Allowing for the presence of noise in our experimental NMR spectra, for purposes of integration and assigning bit values of 1 and 0 we set an uncertainty threshold for integration of 15 percent of the noise amplitude.

The solvent was always deuterated chloroform (Aldrich), the deuterium NMR resonance of the solvent serving for shimming the probe, to provide field/frequency lock as well as an internal reference frequency.

B.1 Approach 1: NAND-based logic gates implemented with DOSY-related experiments

Sample. A sample of chloroform and high vacuum grease in deuterated chloroform.

Pulse sequence parameters. The modified PGSE sequence depicted in figure 6a was used with the following parameter values: τ_d = 0.40105 s, τ_g = 1 ms. Input parameters were set as either 1% or 95% of the gradient strength κ_g; $\tau_{d'} = 0$, or $\tau_{d'} = 69.1\,\mu$s (for a 90° dephasing of the polymethyl siloxane ^{1}H NMR signal). The latter value is calculated from $\Delta\omega_{iso}^{CS} = 3598.4$ Hz. The transmitter frequency was set on-resonance at ω_{iso}^{CS} of chloroform.

B.2 Approach 2a: NOR-based logic gates implemented with selective excitation on a single signal

Sample. A sample of chloroform in deuterated chloroform.

Pulse sequence parameters. The pulse sequence used is depicted at the bottom of figure 11a. The selective pulse had a duration $\tau_p = 80$ ms for a 90° flip angle. The centre of the spectrum was slightly off-set (at -7.25 ppm) from ω_{iso}^{CS} of chloroform, with an offset of the selective pulse of either -18.2 Hz (on resonance) or 6000 Hz (off resonance); and $\tau_d = 0$, or $\tau_d = 13.7$ ms (for a 90° dephasing of the ^{1}H signal, calculated for an offset of -18.2 Hz).

B.3 Approach 2b: NOR-based logic gates implemented with multisite selective excitation

Sample. A mixture of high vacuum grease, acetone, dichloromethane and chloroform in deuterated chloroform.

The half-adder implementation used a sample of chloroform and high vacuum grease in deuterated chloroform.

Pulse sequence parameters. A double pulsed-field-gradient echo sequence was used (figure 6b), where selective pulses had a duration $\tau_p = 20$ms for a 180° flip angle. As the first input, selective pulses were applied either off-resonance (6000 Hz) or on-resonance for each signal (polymethyl siloxane: 1811.6 Hz, acetone: 762.0 Hz, dichloromethane: -806.7 Hz, chloroform: -1797.7 Hz for a spectrum centred at -3.69 ppm). As the second input, the phase of the first set of selective pulses was either $\phi_p = 0^\circ$ or $\phi_p = 45^\circ$ phase shift, whereas the phase of the second set always remained constant. Gradient strengths were $\kappa_{g_1} = 15\%$ for the first gradient echo and $\kappa_{g_2} = 10\%$ for the second.

Identical experimental parameters were used for the implementation of the half-adder circuit.

B.4 Approach 3: NAND-based logic gates implemented with slice-selection experiments.

Sample. A sample of chloroform in deuterated chloroform.

Pulse sequence parameters. The implementation was carried out with a pulse sequence for multiple slice selection (figure 6c). Pulse duration was $\tau_p = 5$ ms for a 180° flip angle. For the two inputs, pulse offsets were set to 700 Hz and -700 Hz, to achieve two peaks separated at the baseline, or to 15000 Hz when no signals were desired. Gradient strengths $\kappa_{g_1} = \kappa_{g_2} = 3\%$ with a rectangular shape. The delay between the activation of the first gradient and application of the 180° selective pulses (τ_d) was set to 0.01s, and the duration of data acquisition was τ_a = 0.023s.